Numerical Quasi Stationary and Transient Analysis of Annular Linear Electromagnetic Induction Pump

L. Goldsteins[*1], L. Buligins[2], Y. Fautrelle[3], C. Biscarrat[1], S. Vitry[1]
[1]Commission of atomic and alternative energies (CEA), University of Latvia (UL), Grenoble Institute of Technology (INPG), [2] University of Latvia (UL), [3] Grenoble Institute of Technology (INPG).
*Corresponding author: France, 13108 Saint-Paul-lès-Durance, Bat. 204, Linards.Goldsteins@cea.fr

Abstract:
In this paper axisymmetric model of annular linear electromagnetic induction pumps using numerical methods and four approaches (two transient and two quasi-stationary) with different complexity is studied. Comparison of integral characteristics is performed between numerical approaches and also with analytic estimations. Distributions of physical parameters over length and height of channel are analyzed and strong influence of higher spatial harmonics is observed. In transient approaches double supply frequency pressure pulsations amplitude is estimated. In the end preferable applications of each method are summarized.

Keywords: Electromagnetic, pump, MHD, transient, coupling.

Symbols used:

$A\ \left[\frac{Wb}{m}\right]$ - magnetic vector potential;
$B\ [T]$ - magnetic field flux (0 - amplitude);
$E\ \left[\frac{V}{m}\right]$ - electric field intensity;
$j\ \left[\frac{A}{m^2}\right]$ - current density (0 – amplitude, l - linear);
$\mu_0\ \left[\frac{T\cdot m}{A}\right]$, magnetic permeability of vacuum ;
$\sigma\ \left[\frac{S}{m}\right]$ - conductivity; s – slip; $t\ [s]$ - time;
$v\ \left[\frac{m}{s}\right]$ – velocity (m – mean, B – magnetic field);
$\eta\ \left[\frac{Pa}{s}\right]$ - dynamic viscosity; $\rho\ \left[\frac{kg}{m^3}\right]$ – density;
$f_{EM}\ \left[\frac{N}{m^3}\right]$ - electromagnetic force density;
$l\ [m]$ - length of channel; $R\ [m]$ – mean radius;
$b\ [m]$ - height of the nonmagnetic gap;
$d_m\ [m]$ - height of liquid metal layer;
$\tau\ [m]$ - half wave length;
$\alpha = \frac{\pi}{\tau}\ \left[\frac{rad}{m}\right]$ - wave number;
$\lambda\ \left[\frac{rad}{m}\right]$- hydraulic resistance coefficient;
$p\ [Pa]$ - pressure; $Q\ \left[\frac{m^3}{s}\right]$ – flowrate;
$f[Hz]$ – frequency (l – reference frequency);
$T = \frac{1}{f}[s]$ - period;
k_w, k_l - coefficients of conducting wall and longitudal effects;

1. Introduction

The transportation of liquid metals poses significant challenge due to the aggressive nature of chemically active (corrosion, oxidation) high temperature media. Electromagnetic (EM) induction pumps are used for liquid metal transportation in variety of technological processes.

Main advantage of such device is contactless pumping of liquid metal using electromagnetic force, therefore hermetic construction can be designed with significant safety improvements over mechanical pumps. Use of annular linear electromagnetic induction pumps (ALIP) is foreseen in Gen IV sodium-cooled fast reactors (SFR) therefore posing interest of this topic.

In present work mainly numerical approaches are used to study and analyze electromagnetic and magnetohydrodynamic (MHD) effects in annular linear electromagnetic induction pump using commercially available software COMSOL. Main attention is paid to physical processes occurring in the liquid metal flow, analyzes of which are important to better understand and characterize phenomena considered as instabilities.

2. Governing equations

MHD problem consists of Maxwell eq. in reduced form [1, 2] (1-4), Ohms law in differential form (5) and Navier – Stokes eq. (6):

$$\begin{cases} \nabla \boldsymbol{E} = 0 \quad (1) \\ \nabla \times \boldsymbol{E} = -\dfrac{\partial \boldsymbol{B}}{\partial t} \quad (2) \end{cases}; \qquad \begin{cases} \nabla \boldsymbol{B} = 0 \quad (3) \\ \nabla \times \boldsymbol{B} = \mu_0 \boldsymbol{j} \quad (4) \end{cases};$$

$$\boldsymbol{j} = \sigma(\boldsymbol{E} + \boldsymbol{v} \times \boldsymbol{B}) \quad (5)$$

$$\rho\left[\frac{\partial \boldsymbol{v}}{\partial t} + (\boldsymbol{v}\nabla)\boldsymbol{v}\right] = -\nabla p + \eta \Delta \boldsymbol{v} + \boldsymbol{f_{EM}} \quad (6)$$

By defining vector potential (7, 8) one can derive so called *Induction eq.* (9) which is EM eq. to be solved (also by COMSOL [3]).

$$\begin{cases} \nabla \times \boldsymbol{A} = \boldsymbol{B} & (7) \\ \nabla \boldsymbol{A} = 0 & (8) \end{cases};$$

$$\Delta \boldsymbol{A} = \mu_0 \sigma \left[\frac{\partial \boldsymbol{A}}{\partial t} - (\boldsymbol{v} \times \nabla \times \boldsymbol{A}) \right] - \mu_0 \boldsymbol{j_e} \quad (9)$$

From (9) it can be easily noticed that:

$$\boldsymbol{j} = \sigma \left[-\frac{\partial \boldsymbol{A}}{\partial t} + (\boldsymbol{v} \times \nabla \times \boldsymbol{A}) \right] \quad (10)$$

Therefore by having solution of vector potential from (9), EM force can be estimated (11) and used in solving (6).

$$\boldsymbol{f_{EM}} = \boldsymbol{j} \times \boldsymbol{B} \quad (11)$$

As system of (6) and (9) is non-linear it can be precisely solved using only iterative methods. However, in praxis so called *solid body* (SB) or *electrodynamic* approximation is often used, neglecting (6) and using only mean velocity of the flow.

3. Simple ALIP model

Basic model of electromagnetic induction pump is so called *ideal machine* (Figure 1).

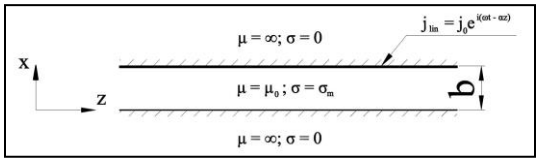

Figure 1. Ideal model of EMIP in Descartes coordinate system.

It consists of two infinite length perfect ferromagnetic plates and between them conductive media, sodium, moves with constant velocity. On surface of upper ferromagnetic plate linear current is applied in harmonic form. For more details on MHD machine theory see [1, 2].

Analytical formula for estimation of quasi stationary (QS) developed pressure using SB approximation is:

$$\Delta p = \frac{\sigma B_0^2 v_B s l}{2} \cdot k_w k_l - \lambda \frac{l}{D_h} \frac{\rho v_m^2}{2} \quad (12)$$

The last part of (12) is pressure losses due to the friction on channel walls. It should be noted that SB approximation works well in integral characteristic estimations. Also it is shown in [2], that influence of cylindrical system curvature on integral parameters is negligible (order of 1 – 2 %) if relations (13) and (14):

$$\frac{R}{b} \geq 2 \ldots 3 \quad (13); \qquad \frac{\tau}{b} \geq 2 \ldots 3 \quad (14)$$

Nevertheless, it was found that due to the fluid secondary circuit, in the case of high magnetic Reynolds number, MHD machine can experience instability [4]. While in the case of ALIP this effect is strongly connected with broken of axial symmetry (not considered in present work), it reminds that hydrodynamic (HD) part can play significant role in such machine and should be taken into consideration.

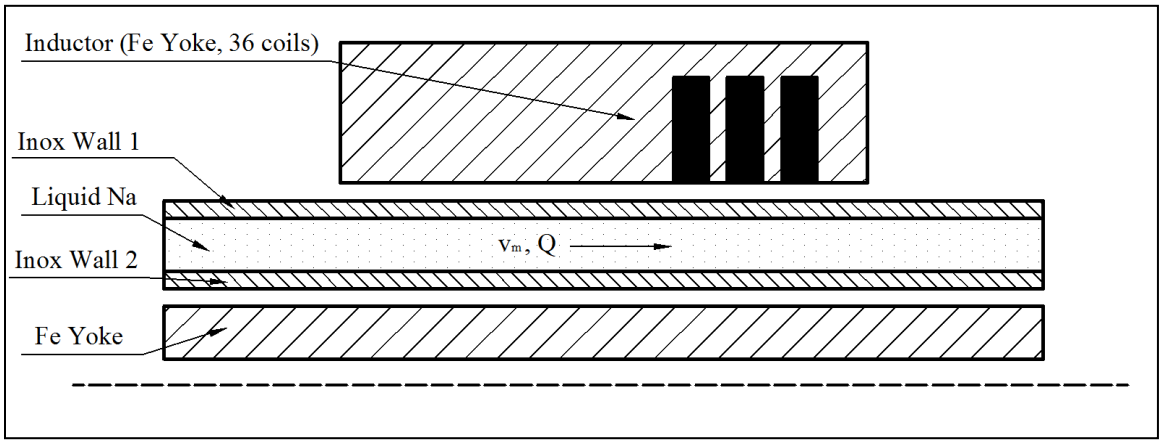

Figure 2. The sketch of axial symmetric ALIP geometry and different zones.

4. Numerical Model

Numerically axisymmetric problem of ALIP was studied using COMSOL 4.3a. Generally, software solves Reynolds averaged Navier-Stokes (RANS) and Induction eq. with some modifications in each particular case [3,5]. Principal sketch of used geometry is shown in (Figure 2).

Problem was solved using four approaches of different complexity:

1. QS SB - QS approach for EM equations, but HD equations aren't solved.
2. Transient SB - Transient approach for EM equations, but HD equations aren't solved with time step: $\Delta t = 0.001$ s.
3. QS MHD – six steps of QS EM equations and stationary HD equations are solved using k – ε turbulence model.
4. Transient MHD – EM and HD equations are solved transiently using k – ε turbulence model with time step: $\Delta t = 0.002$ s.

Example of the used mesh is shown in (Figure 3). It consisted of 131'869 elements, where mapped mesh was used on sodium with 30'000 cells. Cells near channel walls were refined (Figure 4), so that parameter $y^* \leq 11.06$ with most flowrate, which is condition for good wall function approximation [5].

Boundary conditions for HD part on inlet and outlet where set (15), (16) and default wall functions where used. Also in all cases flow as initialized with mean velocity.

$$v|_{inlet} = v_m \quad (15) \qquad p|_{outlet} = 0 \quad (16)$$

Default boundary and initial conditions where used for EM solver and coils where modeled as source of external current density.

In case of transient MHD approach segregated solver was used. It should be noted, that default solver should be slightly modified by segregating vector potential in separate step. It might be also useful to modify time stepping scheme and exclude algebraic degrees of freedom from the evaluation of error in the time-dependent algorithm to improve convergence.

5. Results

All presented results are undimensionlized in a following way (17 – 25):

$$\Delta p' = \frac{\Delta p}{\Delta p_{EM}} \qquad \Delta p_{EM} = \frac{\sigma B_0^2 v_B l}{2} \cdot k_w k_l \quad (17)$$

$$f_z{}' = \frac{f_z}{f_{EM}} \qquad f_{EM} = \frac{\sigma B_0^2 v_B}{2} \cdot k_w k_l \quad (18)$$

$$B_r{}' = \frac{B_r}{B_0} \qquad B_0 = \frac{\mu_0 j_{l,0}}{\alpha b} \quad (19)$$

$$Q' = \frac{Q}{Q_s} \qquad Q_s = 2\pi R b v_B \quad (20)$$

$$v' = \frac{v}{v_m} \qquad v_m = \frac{Q}{2\pi R b} \quad (21) \qquad f' = \frac{f}{f_1} \quad (22)$$

$$t' = \frac{t}{T} \quad (23) \qquad z' = \frac{z}{\tau} \quad (24) \qquad r' = \frac{r}{d_m} \quad (25)$$

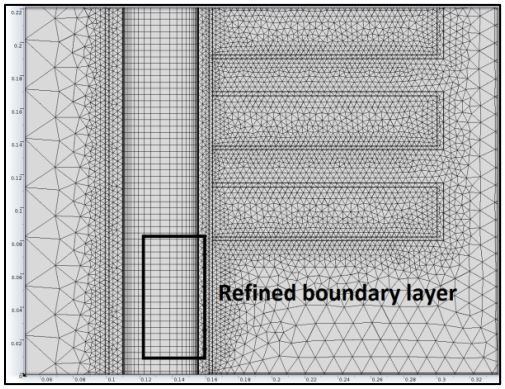

Figure 3. An example of used mesh.

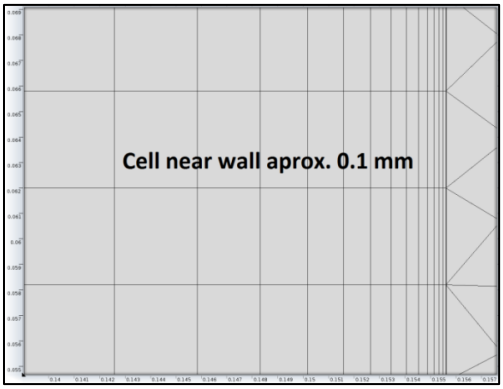

Figure 4. Boundary layer refinement.

In (Figure 5) characteristics of developed EM pressure numerically obtained with QS SB approach (points) using five frequencies are compared with analytical solution considering only main harmonic of height averaged magnetic field. Apparently, analytical results correlate better with numerical solution in case of low flowrate (f' = 3, 4, 5) as well as high flowrate (f' = 1, 2). It could be explained by multi-harmonic structure of magnetic field is not considered in analytic solution.

In (Figure 6) one can observe that in case of higher flowrate distribution of magnetic field near wall 2 (Figure 2) is much more smoother, which means that due to strong interaction with higher (significantly slower) harmonics they are "pushed out of media" (similarities with skin effect). This is confirmed by analyzing axial force along channel, where strong periodic negative force is observed (Figure 7).

In the case of smaller flowrate, developed pressure is mainly determined by main (faster moving) harmonic of magnetic field. One can observe that higher harmonics penetrate better through sodium (Figure 8), due to lower interaction negative effect on axial force is also smaller (Figure 9).

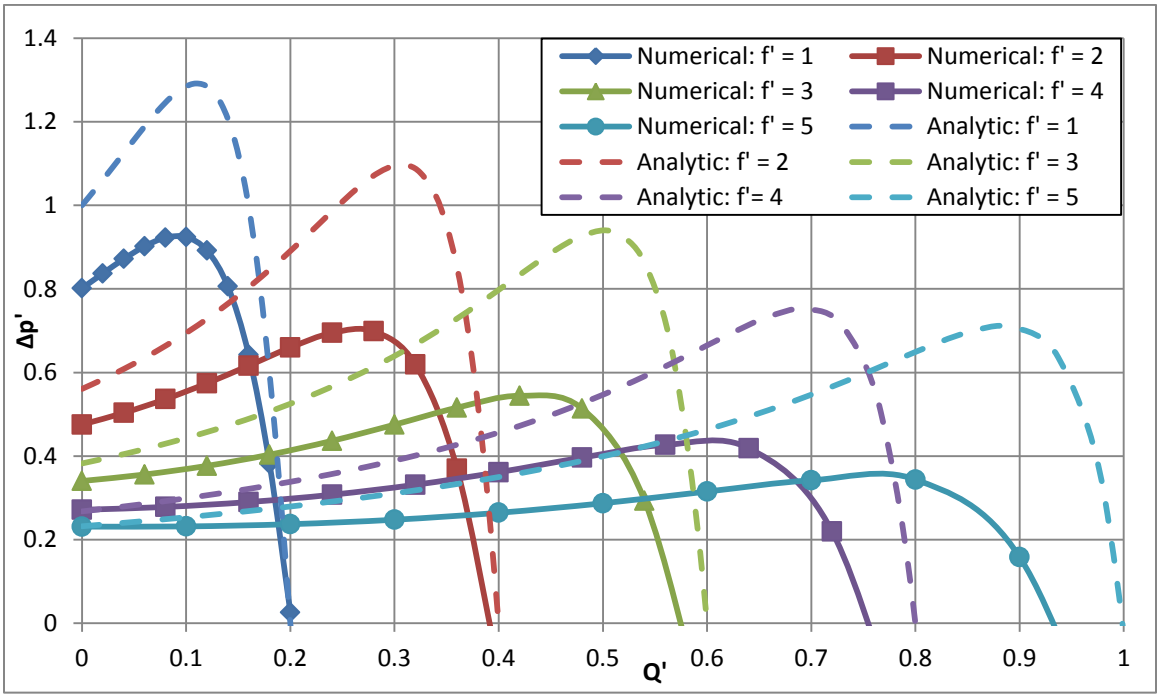

Figure 5. Undimensionlized numerical and analytic p – Q curves of QS SB approximation.

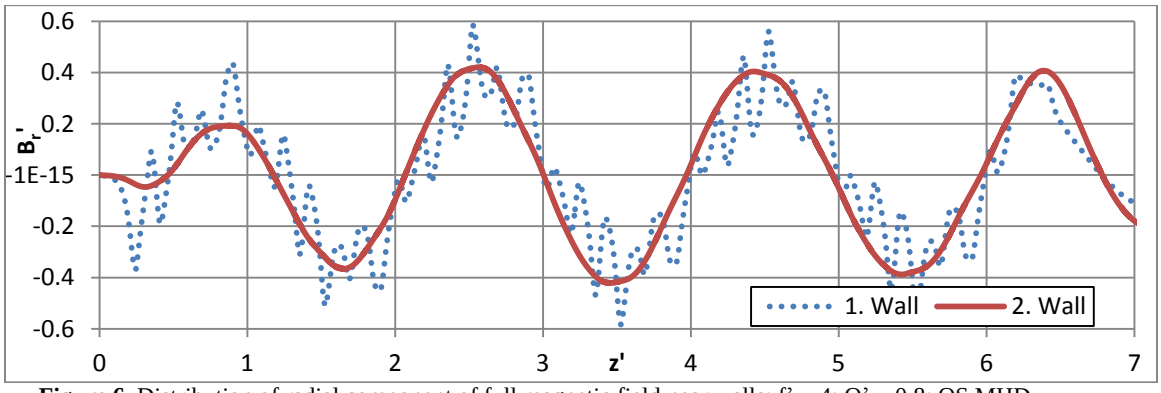

Figure 6. Distribution of radial component of full magnetic field near walls: f' = 4; Q' = 0.8; QS MHD.

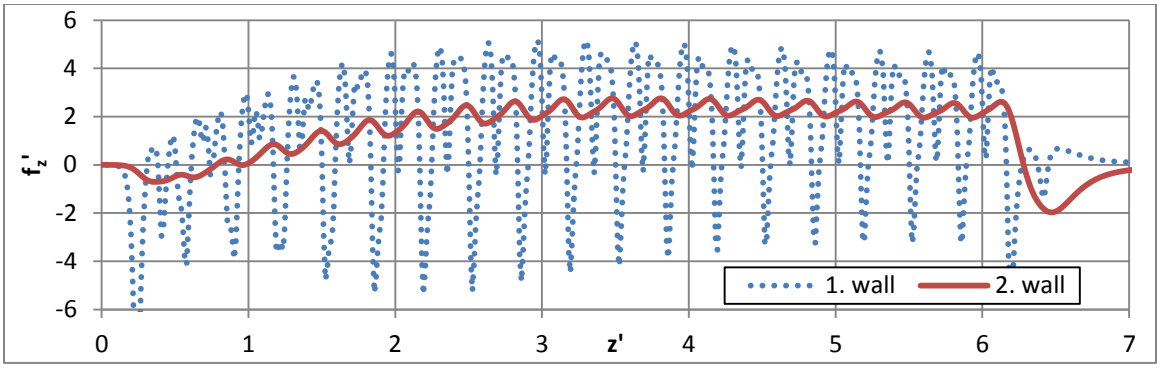

Figure 7. Distribution of axial EM force near walls: f' = 4; Q' = 0.8; QS MHD.

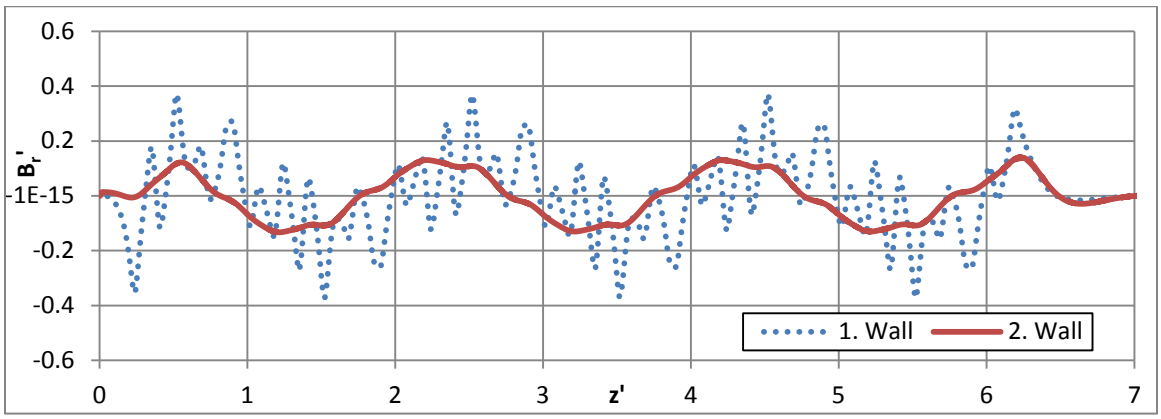

Figure 8. Distribution of radial component of full magnetic field near walls: f' = 4; Q' = 0.2; QS MHD.

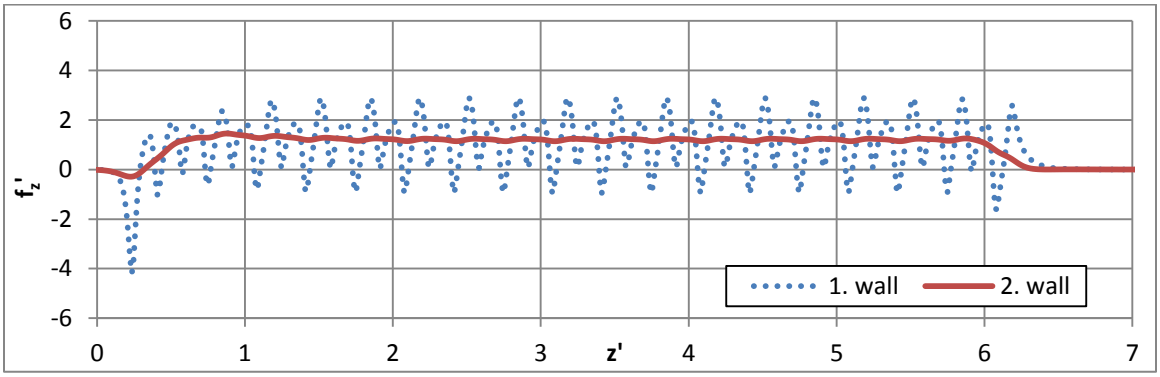

Figure 9. Distribution of axial EM force near walls: f' = 4; Q' = 0.2; QS MHD.

Further study is devoted to influence of fluid nature of media to integral characteristics of such axisymmetric system. Only case f' = 4 is considered.

First of all, developed pressure of QS approaches was compared. Also in the case of QS MHD is possible to estimate difference between EM and developed pressure to calculate pressure losses in channel due to friction which correlates rather well with analytic estimation (Figure 10 secondary axis).

Secondly, transient pressure development is compared in SB and MHD cases. Double supply frequency (DSF) pulsations [6] are observed (Figure 10 error bars, Figures 11, 12) and found that they are rather similar in both cases and time-averaged pressure corresponded very well to one obtained with QS approach.

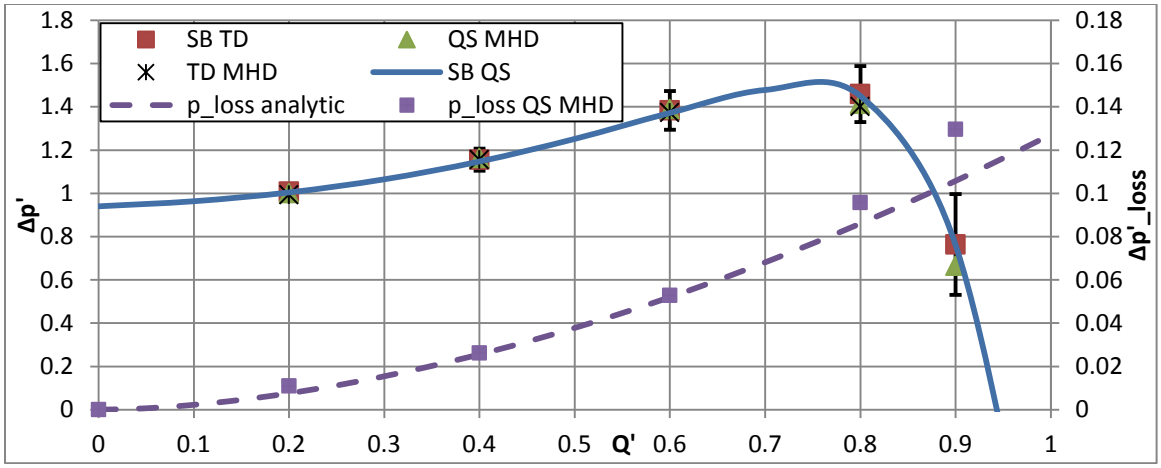

Figure 10. Comparison of time averaged developed pressure and pressure losses: f' = 4; Q' = 0.2; QS MHD.

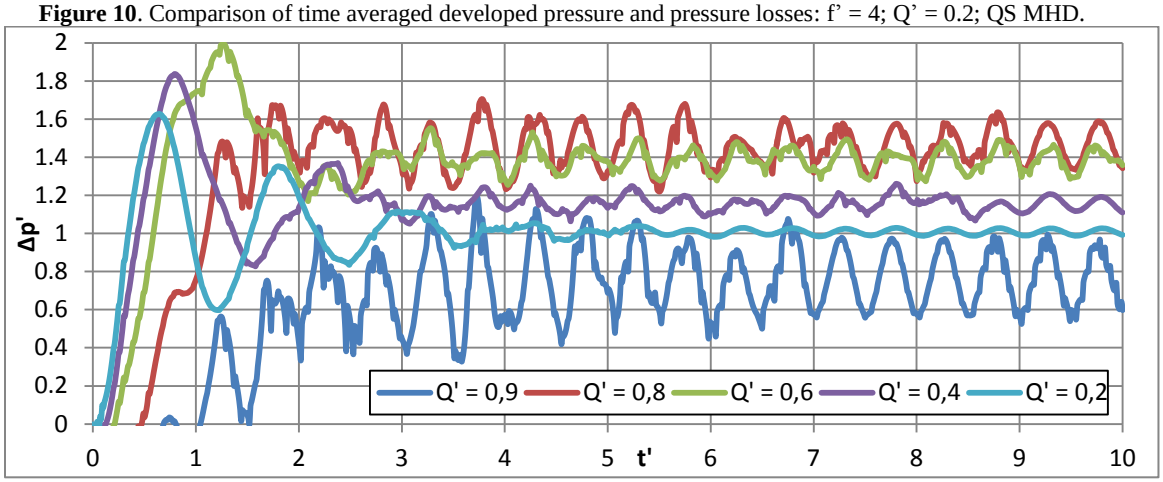

Figure 11. Transient pressure development: f' = 4; Transient SB.

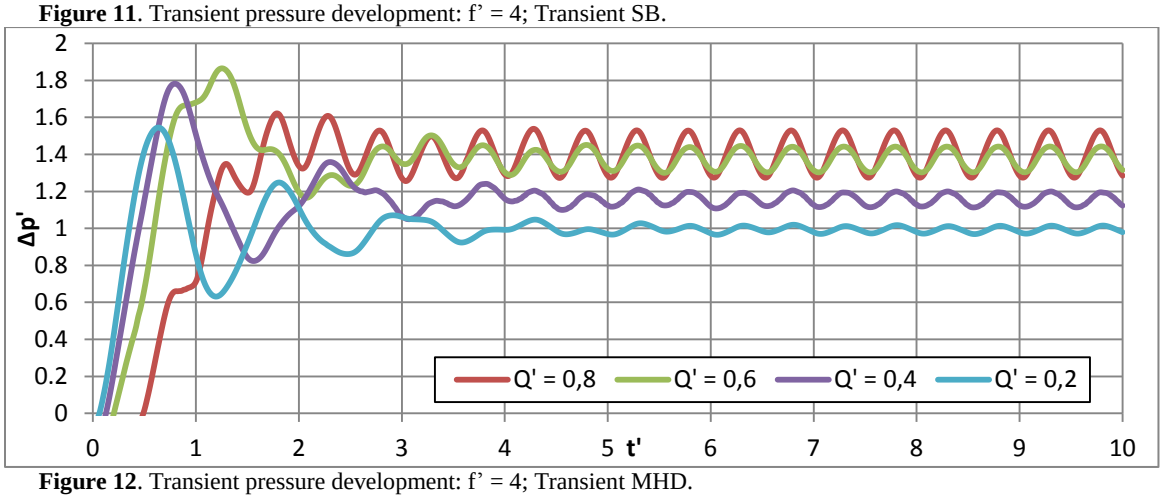

Figure 12. Transient pressure development: f' = 4; Transient MHD.

Lastly, profiles of velocity and axial force just on the edge of tooth in the middle of inductor are analyzed using QS MHD results. Strong negative force near the wall 1 is observed in case of high flowrates, but for low flowrates - force near the same wall is significantly higher than mean value (Figure 13)

It can be observed in (Figure 14) that influence of higher harmonics have negative effect on velocity profile, since near wall 1 velocity is decreased, but wall 2 – increased. Deviations of velocity profile is also strongly connected with ratio of magnetic and inertial forces (Hartmann number) - in case of high flowrates (inertial forces) profile is rather even, while in case of low flowrates it has significant deviations.

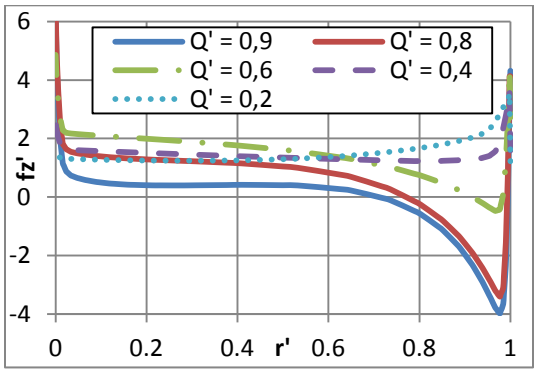

Figure 13. Axial force distribution over channel width: f' = 4; QS MHD.

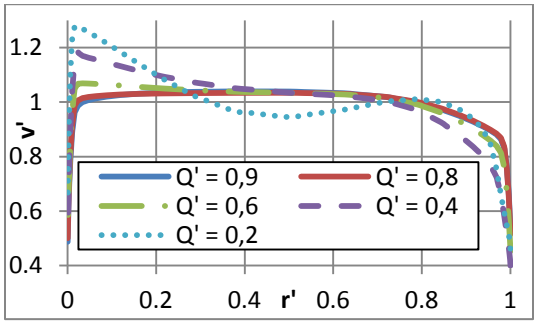

Figure 14. Axial velocity distribution over channel width: f' = 4; QS MHD.

6. Conclusions

Performed analysis reveals that influence of higher harmonics cannot be negligible and have significant impact on integral characteristics (Figure 5), therefore simple analytical model works rather correct only in case of minimal and maximal flowrates. Detailed analysis over length characterizes this effect very well (Figures 6 - 9).

It is estimated that time averaged p – Q characteristic of ALIP in all four approaches are quite the same, therefore simple QS SB approach can be used (Figure 10).

Nevertheless, it is shown that transient SB approach can be successfully used to estimate amplitude of DSF pulsations and is very similar with results obtained with transient MHD approach (Figures 11, 12).

QS MHD approach can be very useful to analyze axial force and velocity profiles more precisely. Significant deviations of velocity profiles are observed over height of channel (Figure 14); however they do not significantly influence integral characteristics (Figure 10). Also this QS MHD approach is used to calculate pressure losses, which correspond quite well with analytic estimations (Figure 10, secondary axis). Lastly, profiles of velocity and axial force just on the edge of tooth in the middle of inductor are analyzed using QS MHD results. Strong negative force near the wall 1 is observed in case of high flowrates, but for low flowrates - force near the same wall is significantly higher than mean value (Figure 13).

Transient MHD approach is most calculation time consuming and should be used if one is interested in time dependent solutions (distributions and profiles). It is shown that using QS MHD and transient SB approach for DSF estimation transient MHD calculation can be successfully substituted.

7. References

1. J. Lielpeters. *MHD machines using liquid metals*, "Zinatne", Riga (1969) (in Russsian)
2. A. Voldek. *Induction magnetohydrodynamic machines with liquid metal working medium*, "Energia", Leningrad (1970) (in Russian).
3. COMSOL AC/DC module Users' guide (2012).
4. A. Gailitis, O. Lielausis. Instability of homogeneous velocity distribution in an induction-type MHD machine. *Magnetohydrodynamics*, **No. 1**, pp. 87 – 101 (1975).
5. COMSOL CFD module Users' guide (2012).
6. H. Araseki, I. R. Kirillov, G. V. Preslitsky, A. P. Ogorodnikov. Double – supply - frequency pressure pulsation in annular linear induction pump. Part I: Measurement and numerical analysis. *Nuclear Engineering and Design*, **No. 195**, pp. 85 – 100 (2000).